NACA

RESEARCH MEMORANDUM

EFFECTS OF SOME LEADING-EDGE MODIFICATIONS, SECTION AND PLAN-FORM VARIATIONS, AND VERTICAL POSITION ON LOW-LIFT WING DRAG AT TRANSONIC AND SUPERSONIC SPEEDS

By Clement J. Welsh, Harvey A. Wallskog, and
Carl A. Sandahl

Langley Aeronautical Laboratory
Langley Field, Va.

NATIONAL ADVISORY COMMITTEE
FOR AERONAUTICS

WASHINGTON

January 18, 1955

NATIONAL ADVISORY COMMITTEE FOR AERONAUTICS

RESEARCH MEMORANDUM

EFFECTS OF SOME LEADING-EDGE MODIFICATIONS, SECTION AND PLAN-FORM VARIATIONS, AND VERTICAL POSITION ON LOW-LIFT WING DRAG AT TRANSONIC AND SUPERSONIC SPEEDS

By Clement J. Welsh, Harvey A. Wallskog, and
Carl A. Sandahl

SUMMARY

Free-flight rocket-propelled model tests have been made to determine the effect of some wing geometry variables on low lift drag at Mach numbers from approximately 0.6 to 2.1. The pertinent results relate to 4- to 7-percent-thick 45° sweptback wings. At supersonic speeds, the wing drag was higher with the NACA 2-006 airfoil sections than with NACA 65A006 airfoil sections particularly at the higher test Mach numbers where it was over 40 percent higher. Drooping the forward 20 percent of the wing 6° increased the wing drag coefficient as much as 30 percent at supersonic speeds. Moving the wing vertically from the fuselage center line to the top of the fuselage increased the configuration drag substantially at supersonic speeds.

INTRODUCTION

The Pilotless Aircraft Research Division has investigated the effects of some wing geometry variables on drag at low lift utilizing rocket-propelled models. The varying wing parameters of the tested configurations included airfoil section, aspect ratio, taper ratio, sweep, wing vertical position and drooped leading edges with and without chord-extended flaps. The results of these tests have been assembled for presentation herein.

The Mach number range of the tests was from approximately 0.6 to 2.1; the Reynolds number range was from approximately 2×10^6 to 29×10^6 based on the wing mean aerodynamic chord. The tests were conducted at the Langley Pilotless Aircraft Research Station at Wallops Island, Va.

SYMBOLS

C_{D_T}	configuration total drag coefficient, $-\frac{2W(a + g \sin \gamma)}{gS\rho V^2}$ (for all models); $-\frac{a_l}{g}\frac{W}{qS}$ (for instrumented models)
C_{D_W}	wing-plus-interference drag coefficient based on total wing area S; $C_{D_T} - C_{D_{body}}$
$C_{D_{W(ex)}}$	wing-plus-interference drag coefficient based on exposed wing area $S_{(ex)}$, $C_{D_W}\left(S/S_{(ex)}\right)$
C_{D_B}	base drag coefficient, $-\frac{(p_b - p)}{q}\frac{A_B}{S}$
C_N	normal-force coefficient, $\frac{a_n}{g}\frac{W}{qS}$
S	wing area (exclusive of chord extensions) obtained by extending leading and trailing edges to center line of model
$S_{(ex)}$	wing area (exclusive of chord extensions) external to fuselage
S_f	maximum fuselage frontal area
c	local chord of basic wing
Λ	sweep of wing quarter-chord line
A	aspect ratio
λ	wing taper ratio
A_B	area of fuselage base
δ_n	deflection of nose flap from wing chord plane in free-stream direction
M	Mach number
a	acceleration tangent to flight path

g	acceleration due to gravity
γ	flight-path angle measured from horizontal
ρ	air mass density
V	velocity tangent to flight path
W	model weight, propellant expended
a_l	longitudinal acceleration
a_n	normal acceleration
p_b	base pressure
p	free-stream static pressure
q	dynamic pressure, $\rho V^2/2$

MODELS

The models have been designated in three general types A, B, and C corresponding to the three types of fuselages used in the investigations as indicated in figures 1 to 4. Wingless models of all three types were also tested. A summary of the wing geometry of the tested configurations is given in table I. Photographs of the model-booster-launcher arrangements are shown in figure 5. A more detailed description of the models follows.

Type A.- Models of type A are illustrated in figures 1 and 4(a). Type A was used specifically for obtaining wing drag and was designed such that the effects of the fuselage on the wing drag tended to be minimized. This type was not instrumented and was propelled by a one-stage booster rocket.

The wing having the extended-chord nose flap as tested on the type A configuration was as indicated in figure 1. The wing sections for the flap portion of the wing were modified such that the forward 40 percent of the initial chord was extended to make the new chord 15 percent greater, and a corresponding change in the thickness ratio for the forward portion of the section such that the section thickness corresponding to the initial 40 percent chord point remained the same.

Type B.- Models of type B, shown in figures 2 and 4(b), were identical to those of reference 1, except for wing geometry. The fuselage was generated by parabolic segments having their vertices at 40 percent of the fuselage length. Fuselage ordinates are given in table II. These models were propelled by an external booster rocket and an internal rocket, and were not instrumented.

Type C.- Type C, shown in figures 3 and 4(c), was a twice-scale version of type B, except for wing geometry and is identical to that of reference 2. The models were propelled by an external booster rocket and an internal rocket, and some of these models were equipped with telemetry. Fuselage ordinates are given in table III.

TEST METHODS

The models were launched from zero-length launchers. During flight, the models were tracked with an NACA modified SCR-584 radar unit to obtain position-time data and with a Doppler radar unit to obtain velocity-time data. Radiosonde equipment was used to obtain the variation of ambient atmospheric pressure, density, and temperature with altitude. In addition, the variation of the wind direction and speed with altitude was obtained by tracking the ascending radiosondes with position radar.

Models C-1, C-2, and C-5 were equipped with NACA telemetry. Measurements included longitudinal and normal accelerations and fuselage base pressure.

The errors are estimated to within the following limits:

C_{D_T}	± 0.0007
M	± 0.005

RESULTS AND DISCUSSION

The variation of Reynolds number with Mach number for the tests is shown in figure 6. The results for each model are given in figures 7, 8, and 9 wherein are plotted total drag coefficient C_{D_T} (based on the total wing area S) and wing-plus-interference drag coefficients obtained by subtracting body drag coefficients (also presented in the figures) from total drag coefficients. The wing-plus-interference drag coefficients C_{D_W} and $C_{D_{W(ex)}}$ are based on total wing area and exposed wing

area, respectively; hence, the difference in the C_{D_W} and $C_{D_{W(ex)}}$ curves is a constant percent difference.

The body drag coefficients were obtained from tests of four-fin wingless models. The decrement in drag coefficient resulting from decreasing the number of tail fins from four to two was obtained from free-flight tests of other fin stabilized models having the subject fins mounted forward on the body in cruciform and planar arrangements. The drag coefficients for the body with two fins so obtained were subtracted from the drag coefficients for the winged two-fin models to obtain wing-plus-interference drag coefficients. It should be noted that this subtractive process renders the wing-plus-interference drag coefficients subject to additional errors when the drag coefficients change rapidly with Mach number (as near $M = 1.0$) because of combined errors in Mach number and drag coefficient.

The base drag coefficients for the type C models and the trim normal-force coefficients for model C-5 (high-wing model) are also presented in figure 9.

Effect of airfoil section.- The results relating to the effect of section on wing drag are assembled in figure 10 wherein wing drag coefficients based on the exposed wing area $C_{D_{W(ex)}}$ are plotted against Mach number. In figure 10(a), it is shown that the drag of the circular-arc airfoil section is larger near $M = 1.0$ than that of the NACA 65-004.2 or the double-wedge airfoil section for sweepback angle of 45°; however, this drag increment approximates the estimated errors of the tests. At the highest Mach numbers investigated ($M \approx 1.5$), the three wings have approximately equal drag.

In figure 10(b) are compared the results for the NACA 65A006 airfoil section and the relatively blunt-nose NACA 2-006 airfoil section. The NACA 2-006 section has the higher drag throughout the test range, and at $M = 2.0$ the drag coefficient is approximately 44 percent higher than that for the NACA 65A006 section.

Effect of wing nose droop and nose flaps.- The effects of wings with nose droop with and without chord-extended flaps are summarized in figure 11. The results for wings with these modifications were obtained with the model trimmed at a small angle of attack. This angle of attack and the trim lift coefficient were estimated to be less than 0.3° and near zero, respectively. The drag coefficients shown are therefore essentially those for zero lift and would probably be slightly lower at a slightly larger lift coefficient. Although the effect of the chord-extended nose flap on the drag of the nose-drooped configuration was not apparent, the results indicate an increase in wing drag coefficient of the order of 20 to 30 percent, for the above wing modifications.

Effect of plan form.- The effect of plan form on total and wing drag coefficients is shown in figure 12. The results at supersonic speeds were as anticipated; decreasing aspect ratio and increasing sweep resulted in lower drag coefficients.

Effect of wing vertical position.- The effect of wing vertical position is shown in figure 13 wherein are compared the forebody drag coefficients (total drag coefficients minus base drag coefficients) for the high-wing configuration of the present report and a similar midwing model (model 6 of ref. 2). The drag coefficients of the high-wing model include a small increment of induced drag (less than 0.0003) resulting from the small trim lift coefficient at which this model flew. The increase in drag coefficient resulting from the high-wing position is substantial, being about 13 percent at the higher supersonic speeds investigated and is consistent with the results of reference 3 for a 60° delta high-wing configuration.

CONCLUSIONS

The results of the present investigation indicate the following conclusions regarding the low-lift drag of 4- to 7-percent-thick 45° sweptback wings at Mach numbers from approximately 0.6 to 2.1:

1. The drag was higher with the blunt-nose NACA 2-006 airfoil section than with the NACA 65A006 airfoil section, particularly at the higher test Mach numbers, where it was over 40 percent higher.

2. Drooping the forward 20 percent of the wing 6° resulted in a 20- to 30-percent increase in wing drag coefficient at supersonic speeds.

3. Moving the wing vertically from the fuselage center line to the top of the fuselage increased the configuration drag substantially at supersonic speeds.

Langley Aeronautical Laboratory,
National Advisory Committee for Aeronautics,
Langley Field, Va., October 18, 1954.

REFERENCES

1. Sandahl, Carl A., and Stoney, William E.: Effect of Some Section Modifications and Protuberances on the Zero-Lift Drag of Delta Wings at Transonic and Supersonic Speeds. NACA RM L53L24a, 1954.

2. Morrow, John D., and Nelson, Robert L.: Large-Scale Flight Measurements of Zero-Lift Drag of 10 Wing-Body Configurations at Mach Numbers From 0.8 to 1.6. NACA RM L52D18a, 1953.

3. Judd, Joseph H.: Flight Investigation of Engine Nacelles and Wing Vertical Position on the Drag of a Delta-Wing Airplane Configuration From Mach Number 0.8 to 2.0. NACA RM L53L21, 1954.

TABLE I

SUMMARY OF TEST CONFIGURATIONS

Model	Aspect ratio	Taper ratio	$\Lambda_{c/4}$, deg	Airfoil section	$\frac{S_f}{S}$	$\frac{S}{S(ex)}$	Comment
A-1	2.15	1.0	0	NACA 65-006	0.006	1.065	
A-2	2.15	1.0	45	NACA 65-004.2	.006	1.065	
A-3	2.15	1.0	45	Circular arc	.006	1.065	t/c = 0.042
A-4	2.15	1.0	45	Double wedge	.006	1.065	t/c = 0.042
A-5	3.57	.30	45	NACA 64(06)A007	.006	1.076	
A-6	3.46	.345	45	NACA 64(06)A007	.006	1.075	Leading edge extended; nose flap deflected 6°; fig. 1
A-7							Wingless model
B-1	4.0	.6	45	NACA 65A006	.061	1.191	
B-2	4.0	.6	45	NACA 65A006	.061	1.191	Nose flap deflected 6°; fig. 2
B-3	4.0	.6	45	NACA 2-006	.061	1.191	
B-4							Wingless model
C-1	3.04	.394	16	NACA 65A003	.061	1.25	
C-2	4.0	.2	45	NACA 65A004	.061	1.280	
C-3	3.0	.2	45	NACA 65A004	.061	1.310	
C-4	3.0	.2	52.5	NACA 65A004	.061	1.300	
C-5	4.0	.6	45	NACA 65A006	.061	1.191	Wing mounted at top of fuselage; fig. 3
C-6							Wingless model

TABLE II

FUSELAGE ORDINATES - TYPE B MODELS

Distance from nose of fuselage, in.	Fuselage radius, in.
0	0
.390	.097
.585	.145
.975	.239
1.950	.469
3.900	.902
5.850	1.298
7.800	1.658
11.700	2.267
15.600	2.730
19.500	3.047
23.400	3.218
27.300	3.248
31.200	3.221
35.100	3.161
39.000	3.069
42.900	2.943
46.800	2.785
50.700	2.594
54.600	2.371
58.500	2.115
62.400	1.826
65.000	1.615

TABLE III

FUSELAGE ORDINATES - TYPE C MODELS

Distance from nose of fuselage, in.	Fuselage radius, in.
0	0
.78	.194
1.17	.289
1.95	.478
3.90	.938
7.80	1.804
11.70	2.596
15.60	3.315
23.40	4.534
31.20	5.460
39.00	6.094
46.80	6.435
54.60	6.496
62.40	6.442
70.20	6.322
78.00	6.137
85.80	5.886
93.60	5.570
101.40	5.188
109.20	4.742
117.00	4.229
124.80	3.652
130.00	3.230

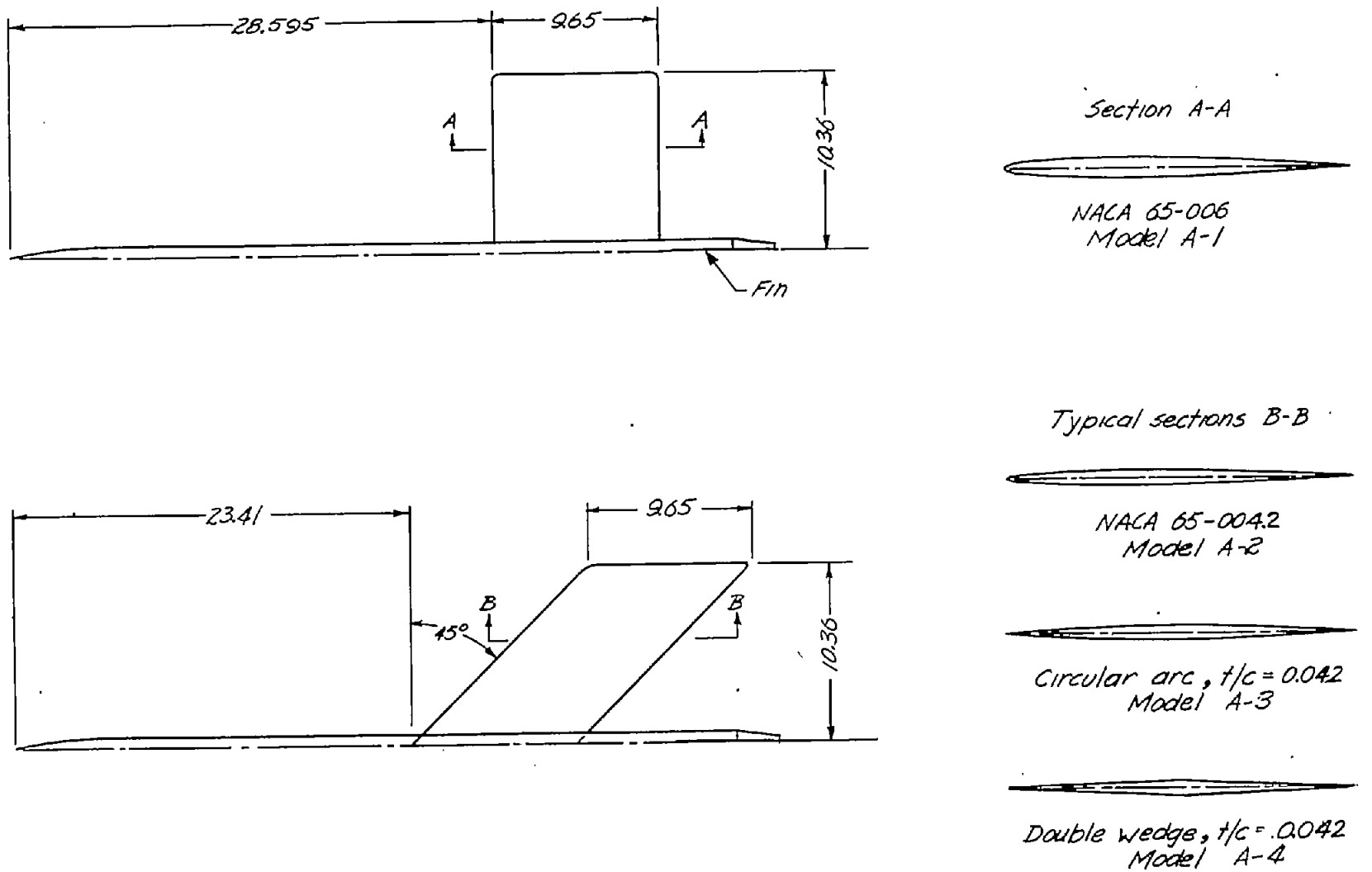

Figure 1.- Geometry of type A models. Linear dimensions are in inches.

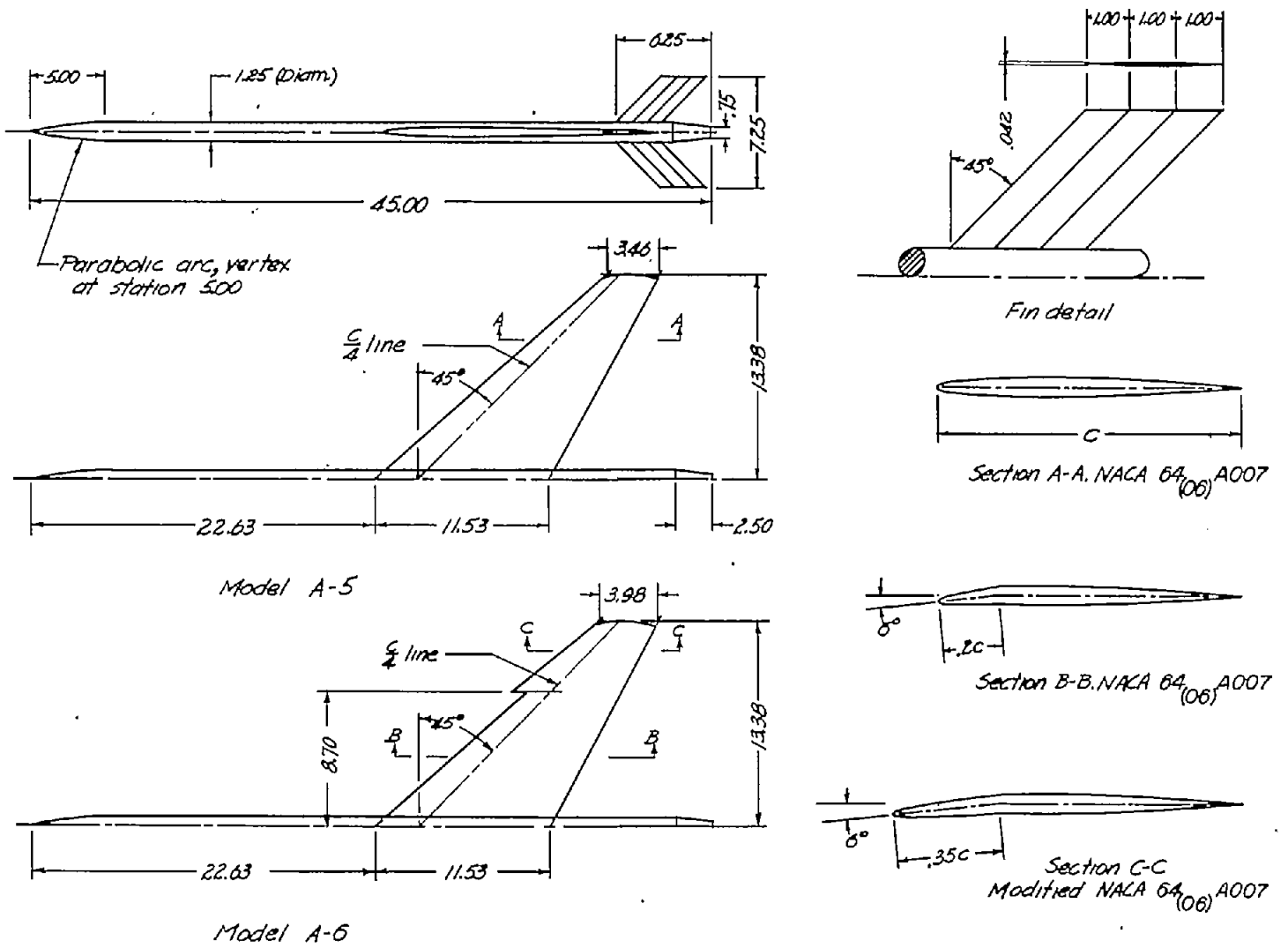

Figure 1.- Concluded.

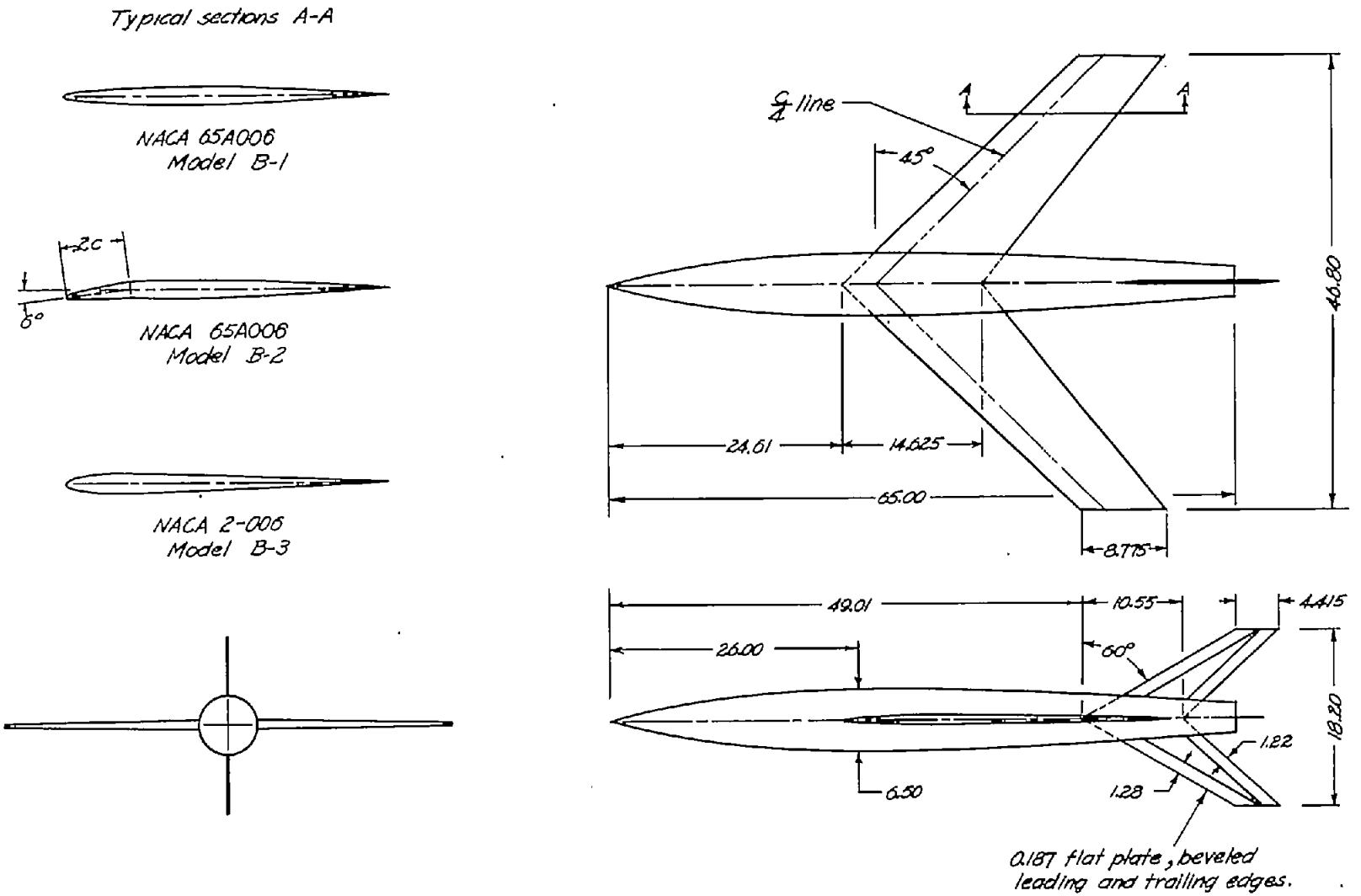

Figure 2.- Geometry of type B models. Linear dimensions are in inches.

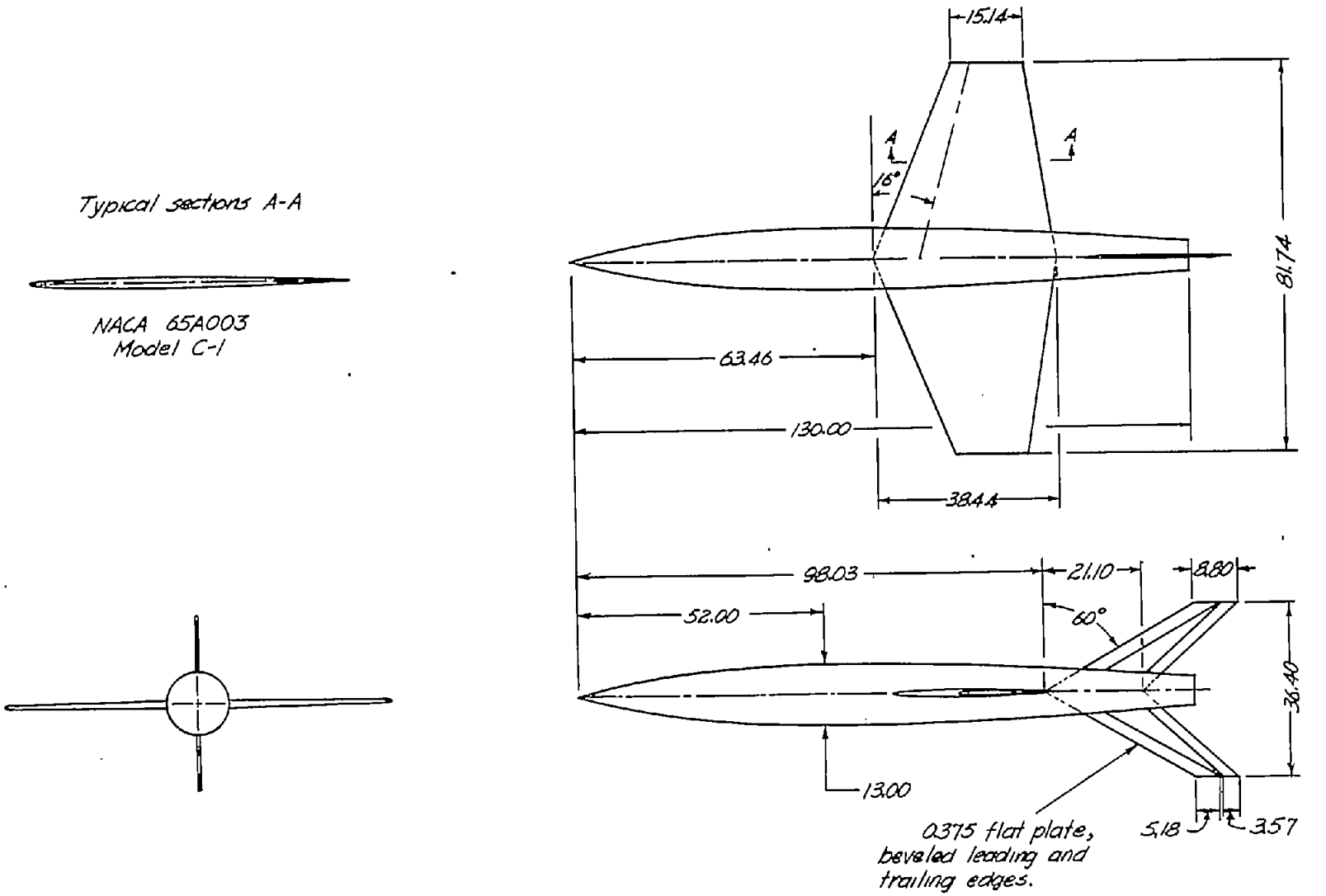

Figure 3.- Geometry of type C models. Linear dimensions are in inches.

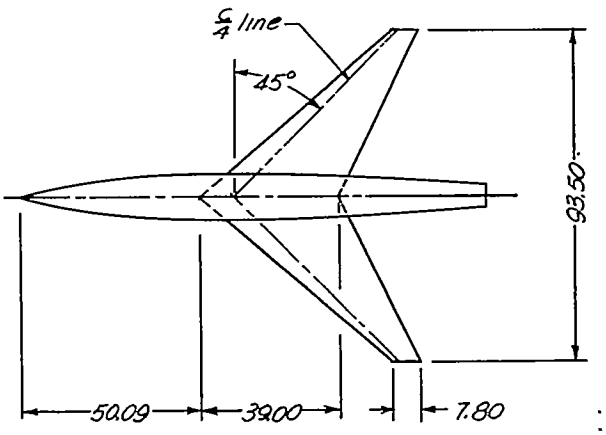

Model C-2

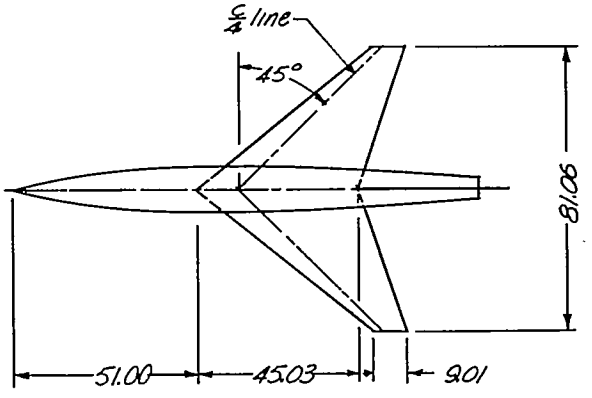

Model C-3

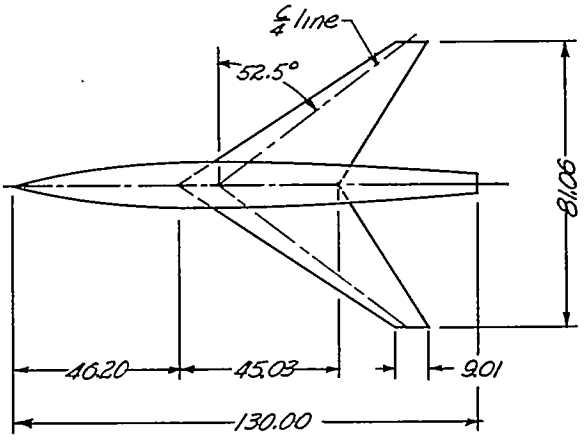

Model C-4

Figure 3.- Continued.

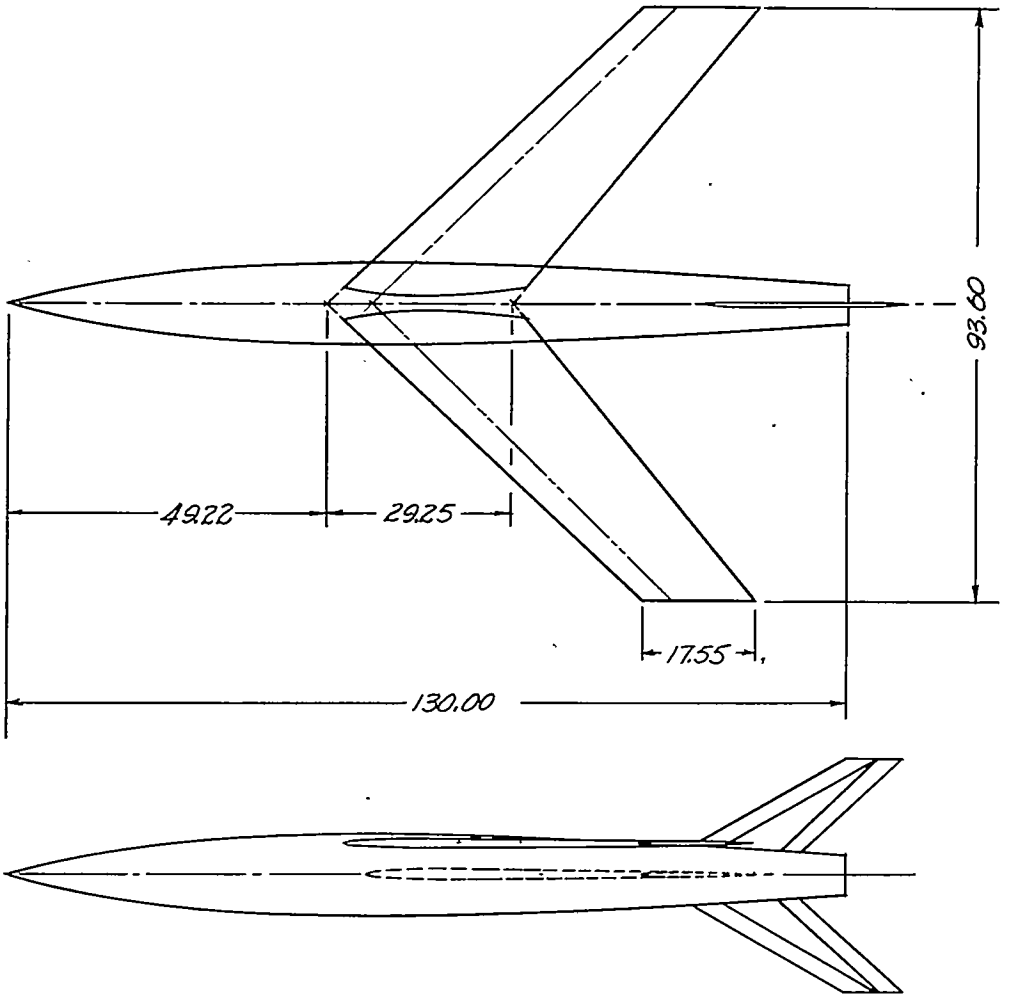

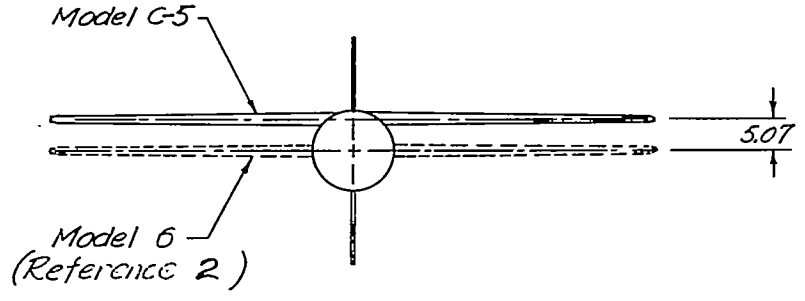

Figure 3.- Concluded.

[redacted]

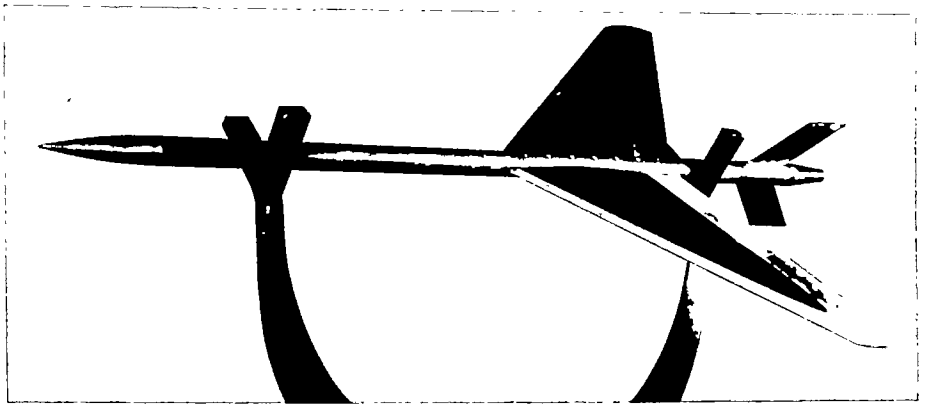

(a) Model A-5. L-77694.1

(b) Model B-1. L-78422.1

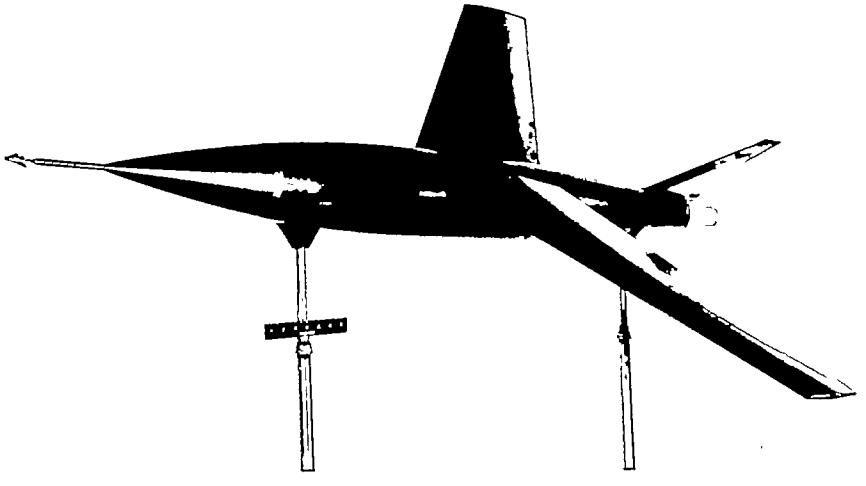

(c) Model C-5. L-76348.1

Figure 4.- Photographs of typical models.

(a) Model A-6. L-78392.1 (b) Model B-3. L-80390.1 (c) Model C-4. L-84402.1

Figure 5.- Photographs of typical model-booster-launcher arrangements.

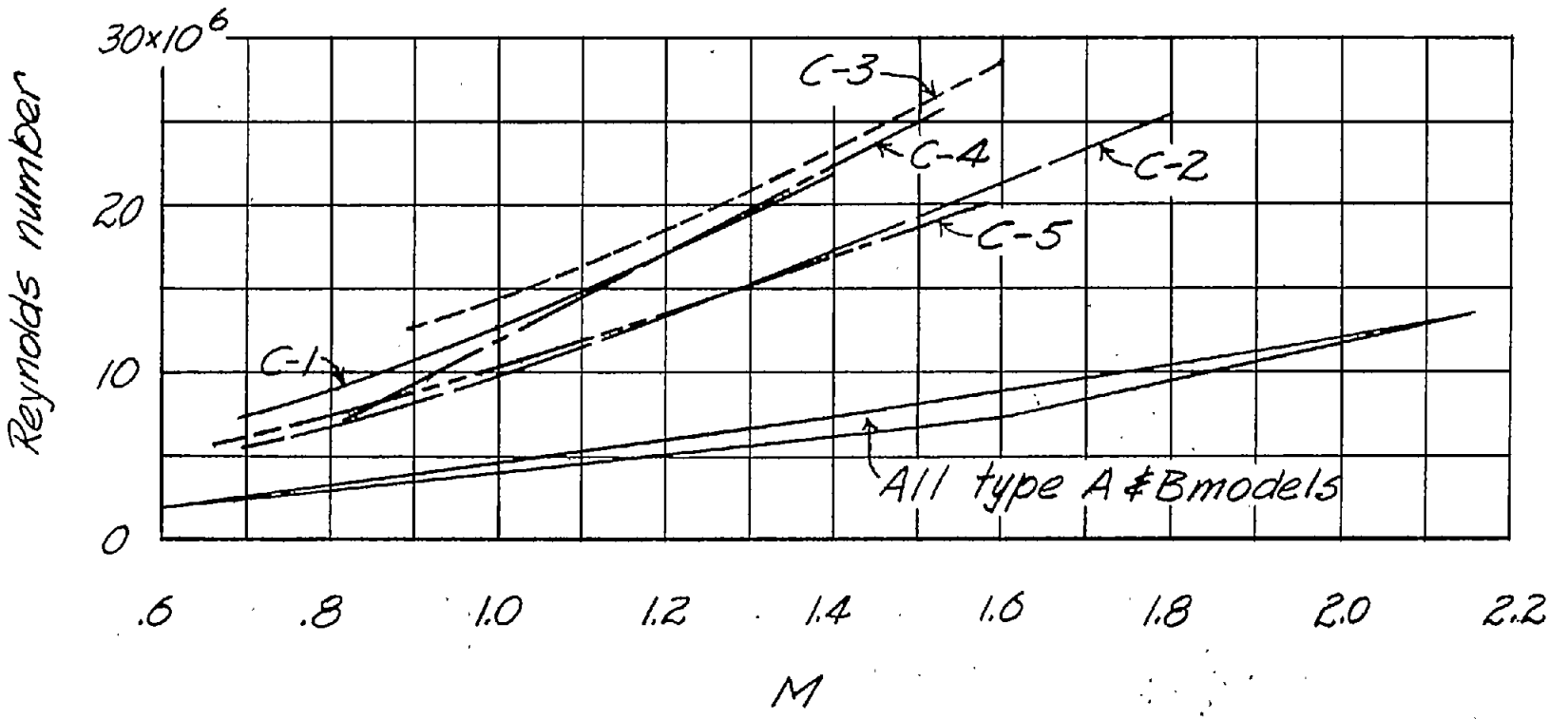

Figure 6.- Variation of Reynolds number, based on wing mean aerodynamic chord, with Mach number.

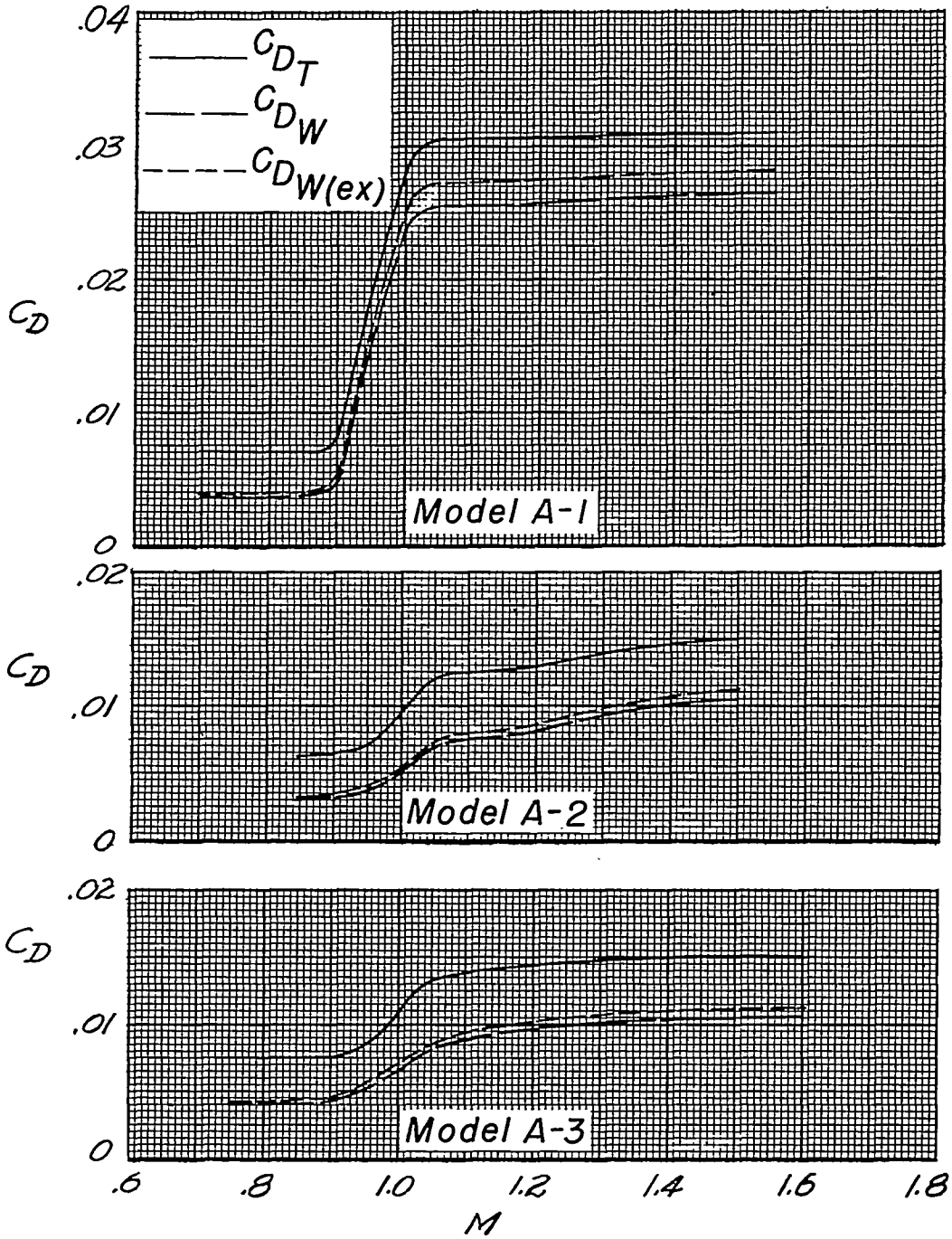

Figure 7.- Test results. Type A models.

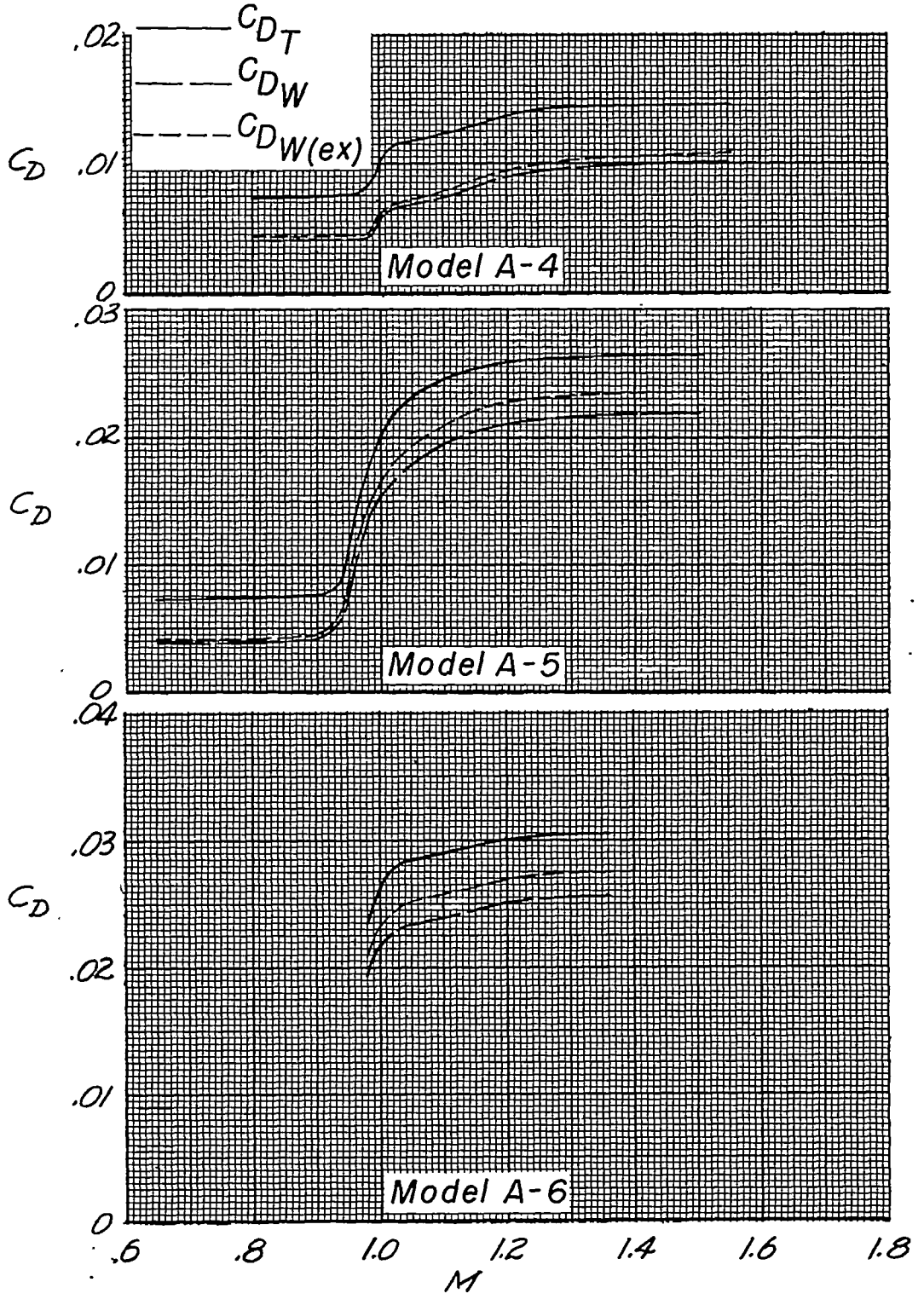

Figure 7.- Continued.

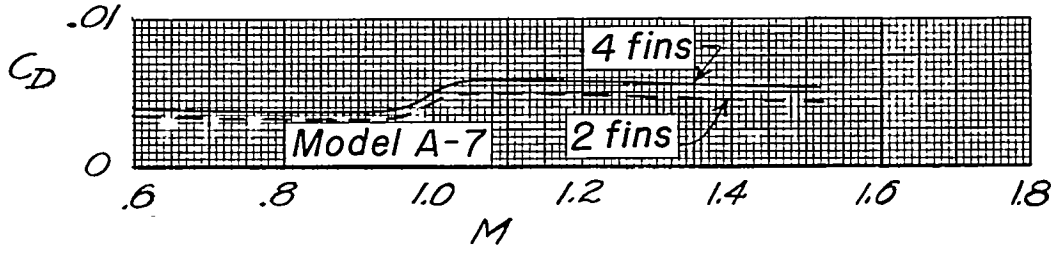

Figure 7.- Concluded.

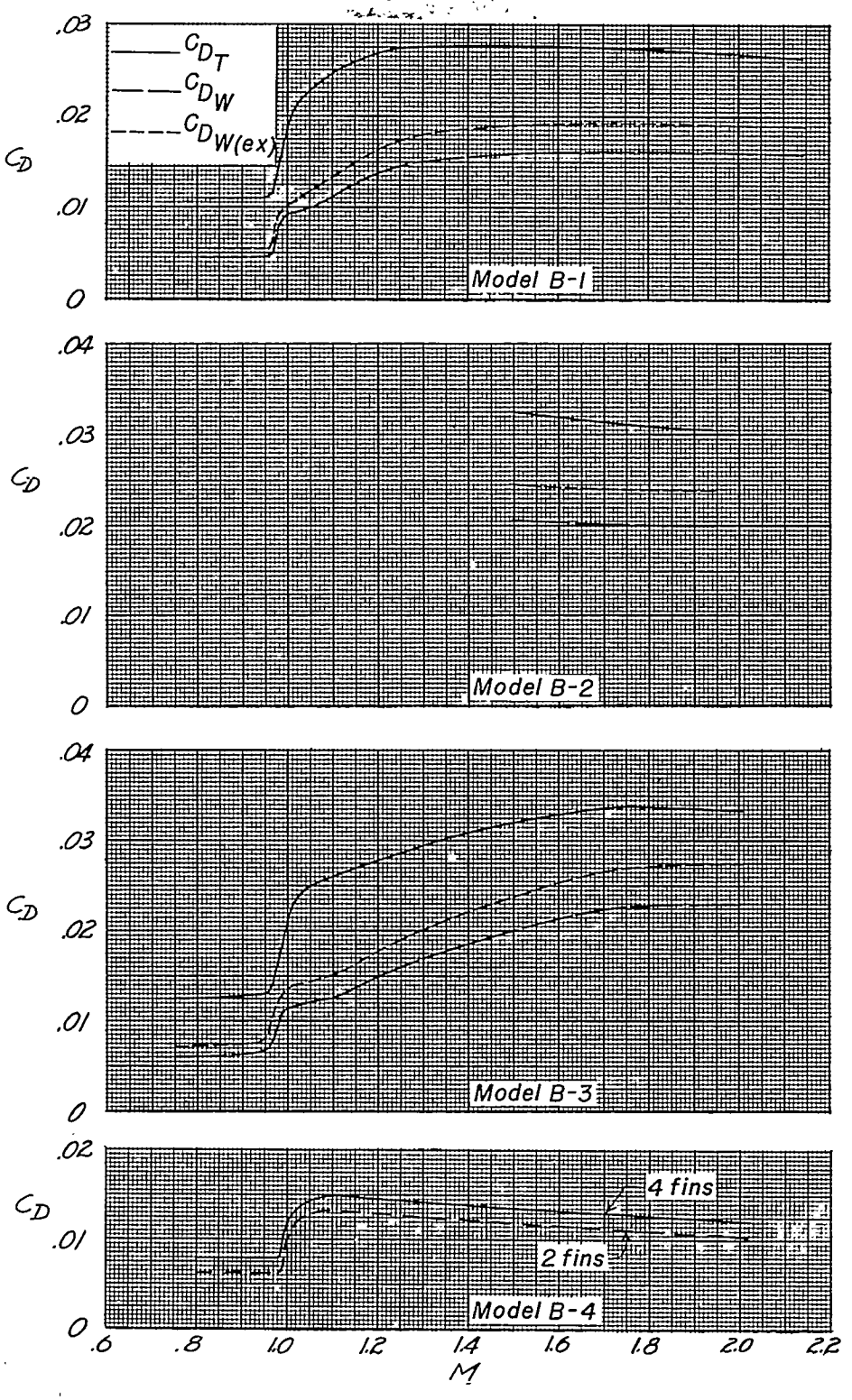

Figure 8.- Test results. Type B models.

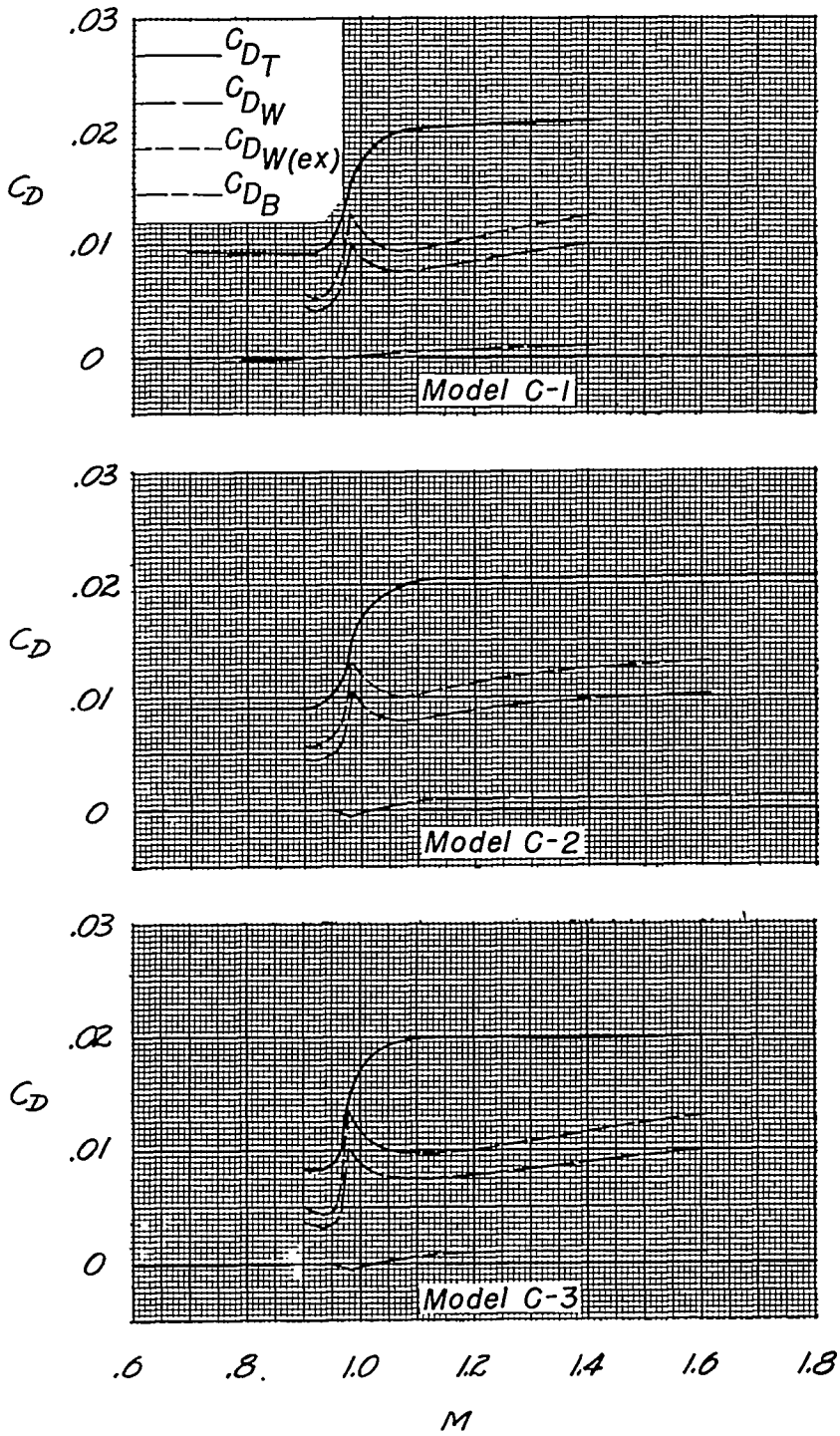

Figure 9.- Test results. Type C models.

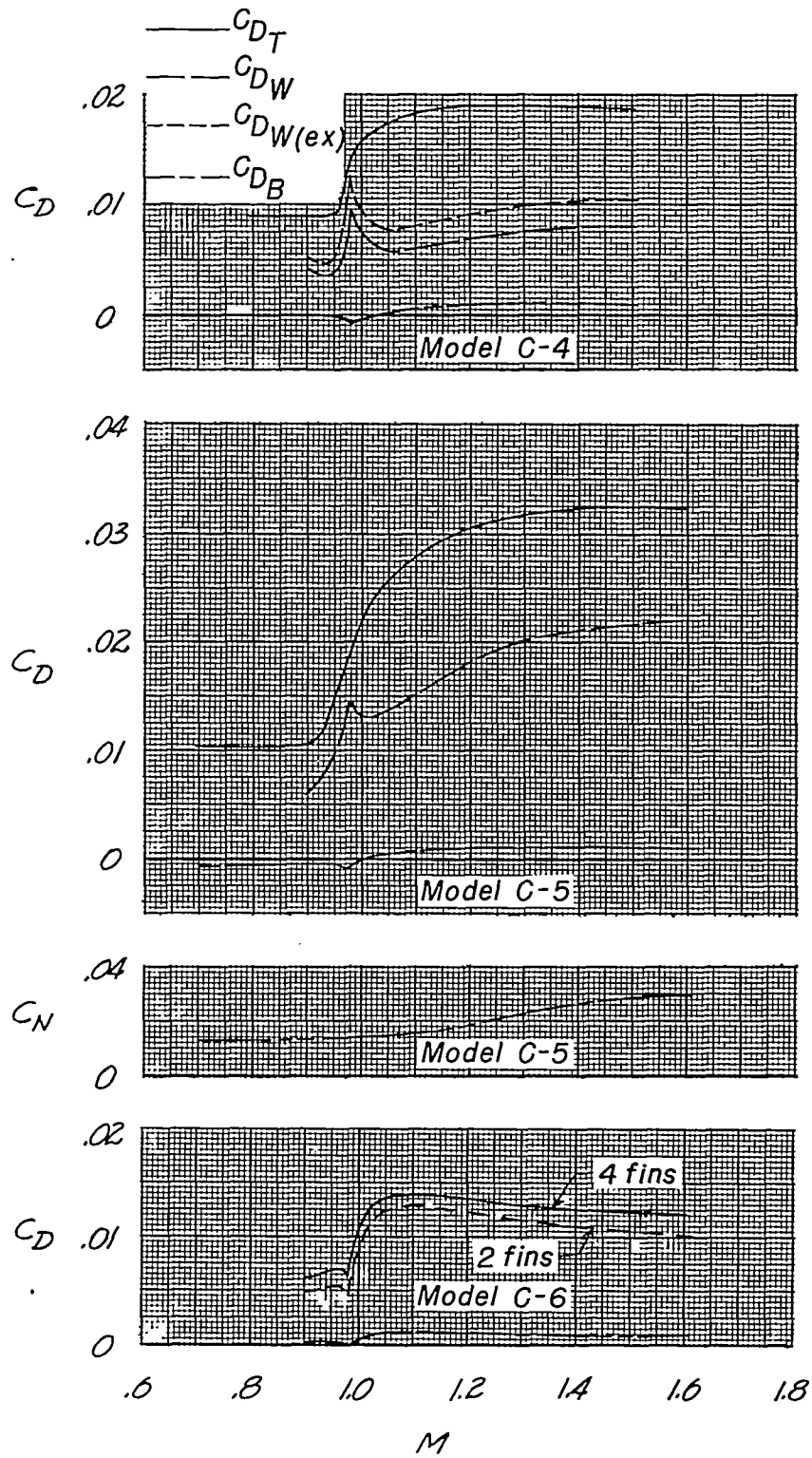

Figure 9.- Concluded.

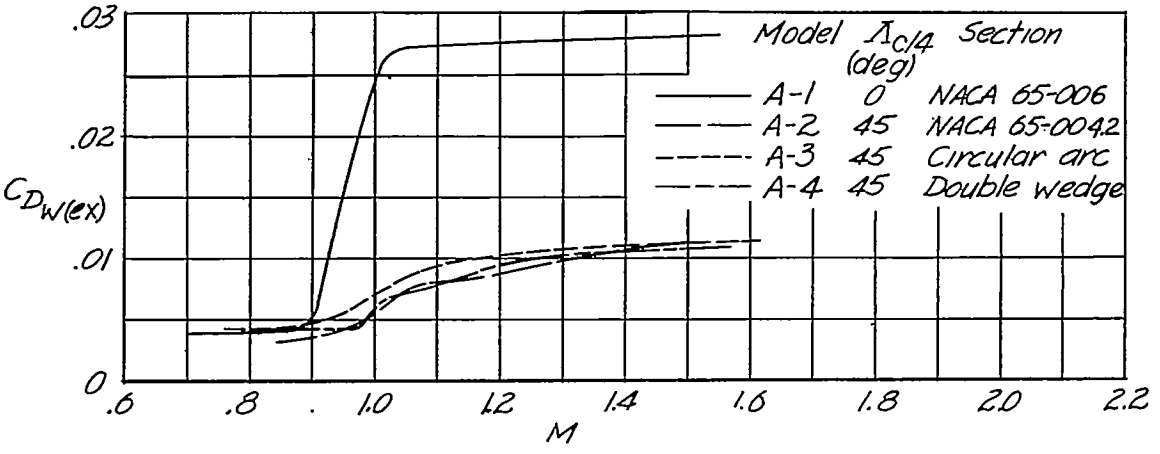

(a) Type A models. A = 2.15; λ = 1.0; thickness ratio = 0.042 unless listed otherwise.

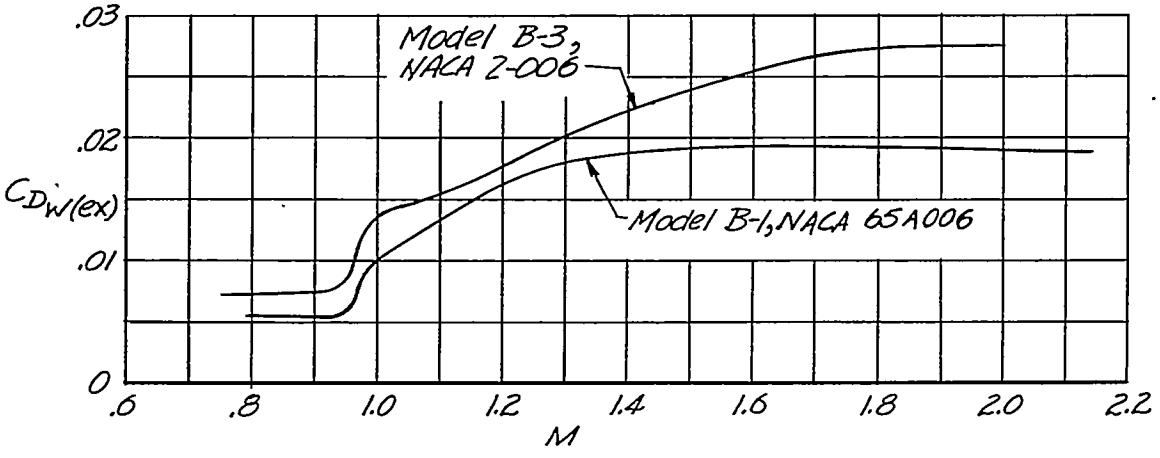

(b) Type B models. A = 4.0; $\Lambda_{c/4} = 45^{\circ}$; λ = 0.6.

Figure 10.- Effects of airfoil section. Airfoil sections are parallel to model center line.

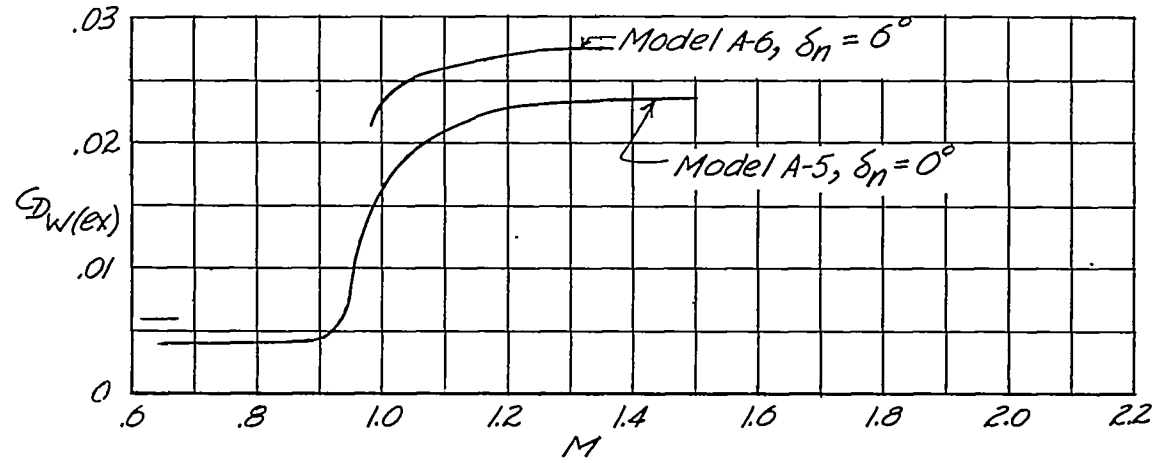

(a) Type A models. A = 3.57; $\Lambda_{c/4} = 45°$; $\lambda = 0.3$. NACA $64_{(06)}$A007 airfoil sections.

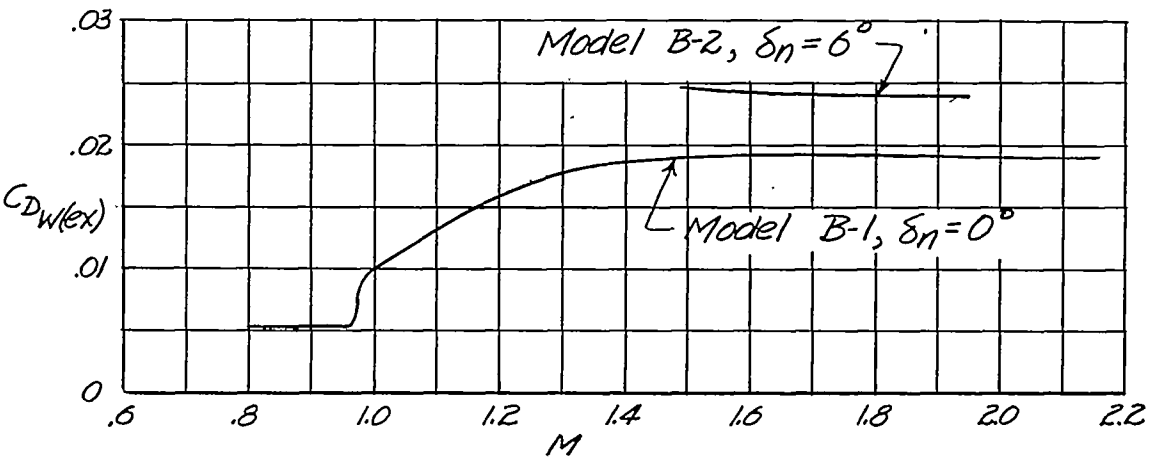

(b) Type B models. A = 4.0; $\Lambda_{c/4} = 45°$; $\lambda = 0.6$; NACA 65A006 airfoil sections.

Figure 11.- Effect of nose flap deflection.

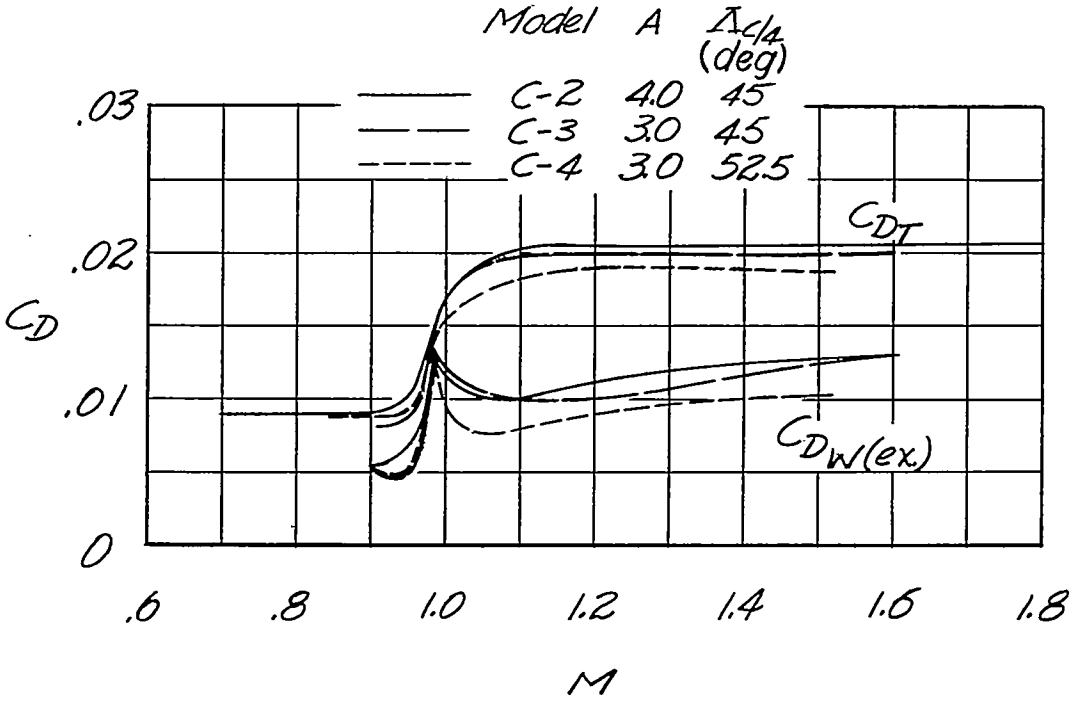

Figure 12.- Effect of plan form. $\lambda = 0.2$; NACA 65A004 airfoil sections.

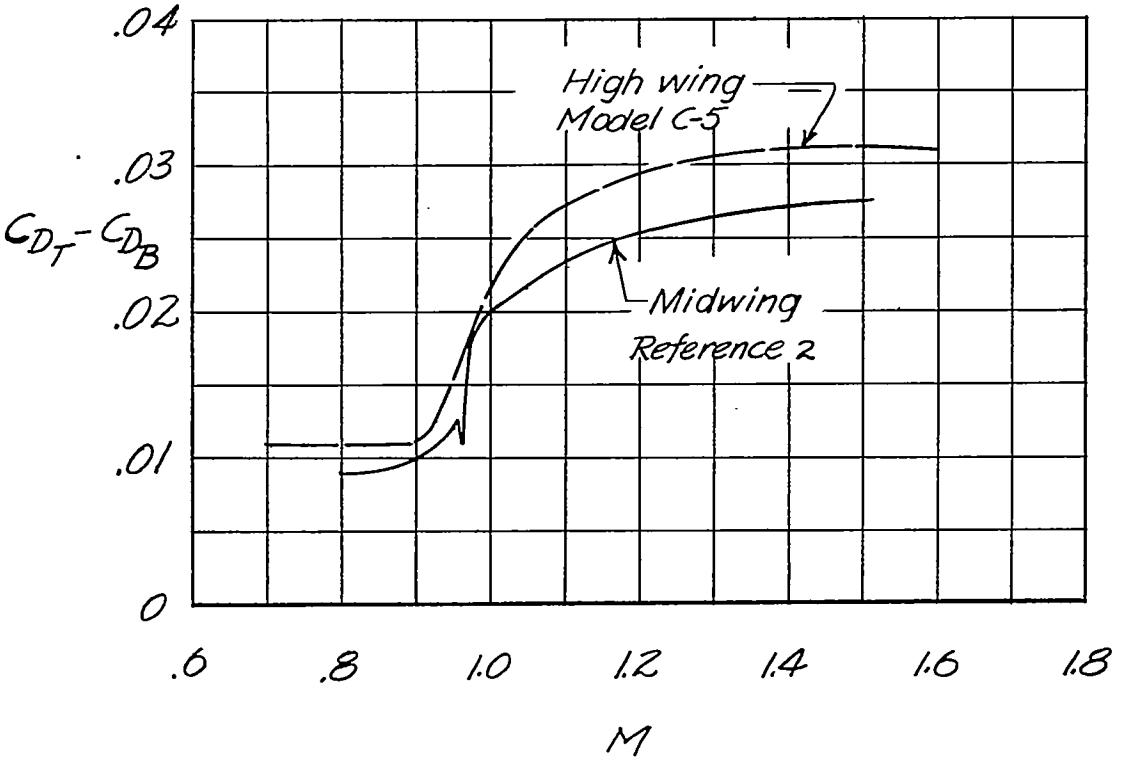

Figure 13.- Effect of wing vertical position. $A = 4.0$; $\Lambda_{c/4} = 45^\circ$; $\lambda = 0.6$; NACA 65A006 airfoil sections.

NACA-Langley - 1-18-55 - 350